

DEVELOPMENT OF OPTICAL FIBER FREQUENCY AND TIME
DISTRIBUTION SYSTEMS*

George Lutes
Jet Propulsion Laboratory, Pasadena, California

ABSTRACT

The Jet Propulsion Laboratory is engaged in the development of ultra stable optical fiber distribution systems for the dissemination of frequency and timing references. The ultimate design goals for these systems are a frequency stability of 10^{-17} for $\tau \geq 100$ sec and time stability of ± 0.1 ns for 1 year and operation over distances ≥ 30 km. This paper will review last years report, describe a prototype system being implemented and discuss progress made in the past year.

INTRODUCTION

Preliminary work on an optical fiber reference frequency distribution system was reported at last year's PTTI conference. This paper is a progress report on this effort and will begin with a brief review, followed by a description of the prototype system and progress made in the last year.

REVIEW

It was reported at last year's PTTI conference that a 3-km experimental multimode optical fiber link operating at 850 nm wavelength was installed at JPL. It was to be used in the development of ultra-stable frequency and timing distribution systems.

The link was stabilized using the conjugation method, reference 1, and achieved a stability of 4×10^{-15} for $\tau = 100$ seconds.

Several problems with this link were reported. The stability was limited by the optical transmitters and receivers. Delay changes as a result of bending multimode fibers are nonreciprocal under some circumstances, and excessively large. This precludes their use for frequency

* This paper presents the results of one phase of research carried out at the Jet Propulsion Laboratory, California Institute of Technology, under Contract No. NAS 7-100, sponsored by the National Aeronautics and Space Administration.

and time reference distribution in non-stationary environments. The minimum loss in optical fibers operating at 850 nm wavelength is about 3 dB/km, which is too large to achieve a 30 km operating distance. The bandwidth of currently available multimode fibers, about 1.5 GHz-km, is not adequate for this use over these distances.

It was concluded in last year's report that, although the results obtained were encouraging, there was still a lot of work to be done.

PROTOTYPE SYSTEM

A prototype system, 8 km in length, will be installed between two stations in the Deep Space Communications Complex (DSCC) at Goldstone, California. It will be a single-mode fiber system and will operate at 1300 nm wavelength. The conjugation type of stabilization that will be used in this system will be an improved version of the one used in the experimental system reported last year.

The goal for frequency stability for distances up to 30 km is shown in Figure 1. With this stability the distribution system will not excessively degrade the stability of future frequency references having a stability of up to 10^{-17} for $\tau = 100$ seconds.

The time distribution stability goal is ± 0.1 ns for 1 year. This goal has not yet been addressed in detail because it can probably be met with minor additions to the frequency distribution system. In any case, most of the problems will have been resolved in the implementation of the more difficult frequency distribution system.

Another goal, not directly related to frequency and timing distribution, is the capability to distribute 400 MHz bandwidth IF signals over 20 km. This goal will be met as a consequence of the frequency and timing distribution work.

These goals can be approached using single-mode optical fibers operating at 1300 nm wavelength. The delay through such fibers is affected very little by bending and the modulation bandwidth is much wider than that of multimode fibers. Also, 1300 nm is near the wavelength which gives minimum dispersion (equivalent to the widest bandwidth) and lowest loss (≤ 1 dB/km).

A block diagram of the system is shown in Figure 2. In this system, a signal is sent to the far end of the cable where it is turned around and returned to the near end. The transmitted signal, $\sin(\omega t + \tau)$, is forced by the control circuit to be the conjugate of the return signal, $\sin(\omega t - \tau)$. Since the forward and return paths have equal delays - being the same path - the phase at the far end of the cable is halfway between the transmitted phase and the return phase or ωt . The phase of

the input reference is also ωt , therefore the phase at the output is the same as the phase at the input.

In Figure 3 the calculated signal-to-noise ratio (S/N) (reference 2) for such a system is shown as a function of the loss in the cable. An operating frequency of 100 MHz and a bandwidth of 10 Hz are assumed. The calculations are supported by measurements made on the 3-km experimental link. The difference between single-mode and multimode fibers is due to greater signal loss in multimode fibers caused by dispersion.

The cable connecting the two stations will contain two single-mode and two multimode optical fibers designed to operate at 1300 nm wavelength. These fibers will be used to develop frequency and timing distribution systems and wideband communications systems. The cable will also contain two multimode optical fibers designed to operate at 850 nm wavelength which will be used for utility communications services between the two stations. The cable will be received in 1- or 2 km lengths and will be plowed into the ground to a depth of 1.5 meters.

The degradation of the stability of a frequency reference signal passing through this cable, without stabilization, has been estimated as follows.

The stability of frequency references is specified at JPL in terms of the square root of the Allan variance (reference 3). The algorithm for computing it is:

$$\sigma = \frac{1}{\sqrt{2} \omega_0 \tau} \sqrt{\frac{1}{N} \sum_{n=1}^N (f_n - f_{n+1})^2}, \quad (1)$$

where:

f_n = average frequency in the interval between t_n and t_{n+1}

f_{n+1} = average frequency in the interval between t_{n+1} and t_{n+2}

t_n = the n^{th} sampling time

τ = the interval between samples,

ω_0 = the nominal angular frequency and,

N = the number of samples of $(f_n - f_{n+1})$.

Only the degradation caused by ambient temperature variations will be considered since this is the predominate source of instability. We consider first sinusoidal variations in temperature and then a step change in temperature.

Assume that a perfectly stable reference frequency is disseminated over a long single-mode optical fiber cable which is buried in the ground. Also assume that the cable is buried deeply enough that the diurnal change in temperature is essentially sinusoidal.

At time (t) the varying component of temperature (T) of the cable is,

$$T = T_p \sin \omega t \quad (2)$$

where

T_p = the peak temperature variation,

P = the period of one cycle of the temperature variation and

$\omega = \frac{2\pi}{P}$ = the frequency of the temperature variation.

The delay (β) in radians through the transmission line as a function of temperature is,

$$\beta = \frac{\omega_0 l}{v} + \frac{\omega_0 l \alpha T}{v} \quad (3)$$

where

$\frac{\omega_0 l}{v}$ = the delay at the mean temperature in radians,

ω_0 = the nominal angular frequency of the disseminated signal,

l = the length of the line in meters,

v = the velocity of propagation in the line ($\approx 2.1 \times 10^8$ m/s for optical fiber) and,

α = the cable's temperature coefficient of delay
 $(\approx 10^{-5}/^{\circ}\text{C})$.

The phase (β) as a function of time (t) is from (2) and (3),

$$\beta = \frac{\omega_0 l}{v} + \frac{\omega_0 l \alpha T_P}{v} \sin \omega t. \quad (4)$$

The average frequency (f) over a time interval (τ) is the total phase accumulated (β_A) during the time interval divided by the time interval (τ),

$$f = \frac{\beta_A}{\tau} \quad (5)$$

Therefore from (4) and (5), the average frequency (f_n) in the interval ($t_n, t_n + \tau$) is

$$f_n = \left[\frac{\beta(t)}{\tau} \right]_{t_n}^{t_n + \tau} = \frac{1}{\tau} \left[\frac{\omega_0 l}{v} + \frac{\omega_0 l \alpha T_P}{v} \sin \omega t \right]_{t_n}^{t_n + \tau} \quad (6)$$

and the average frequency (f_{n+1}) in the next interval ($t_n + \tau, t_n + 2\tau$) is,

$$f_{n+1} = \left[\frac{\beta(t)}{\tau} \right]_{t_n + \tau}^{t_n + 2\tau} = \frac{1}{\tau} \left[\frac{\omega_0 l}{v} + \frac{\omega_0 l \alpha T_P}{v} \sin \omega t \right]_{t_n + \tau}^{t_n + 2\tau}. \quad (7)$$

The absolute value of the difference between these average frequencies is from (6) and (7),

$$\begin{aligned}
|f_n - f_{n+1}| &= \left| \frac{\omega_0 \lambda \alpha T_P}{v\tau} \left[2 \sin \omega (t_n + \tau) - \sin \omega t_n - \sin \omega (t_n + 2\tau) \right] \right| \\
&= \left| \frac{4\omega_0 \lambda \alpha T_P}{v\tau} \left[\sin^2 \frac{\omega\tau}{2} \sin \omega (t_n + \tau) \right] \right|. \tag{8}
\end{aligned}$$

Then, from (1) and (8), the square root of the Allan variance of a signal passing through a transmission line having a sinusoidal variation in delay becomes,

$$\sigma = \frac{4\lambda\alpha T_P}{\sqrt{2}\tau v} \sqrt{\frac{1}{N} \sum_{n=1}^N \left[\sin^2 \frac{\omega\tau}{2} \sin \omega (t_n + \tau) \right]^2}. \tag{9}$$

This equation is evaluated in Figure 4, for values of τ from 1 second to 10^6 seconds and variables $\lambda = 10^4$ meters, $\alpha = 10^{-5}/^\circ\text{C}$, $T_P = 1^\circ\text{C}$, $v = 2.1 \times 10^8$ meters per second and $\omega = 2\pi/86400$ radians per second (diurnal variation). These are realistic values based on measurements made at JPL and at the Goldstone Deep Space Complex.

Now consider a cable that is subjected to a step change in ambient temperature. The change is assumed to be much faster than the time constant of the cable. The relative temperature (T) of the cable at time (t) is,

$$T = T_S \left(1 - e^{-t/\tau_c} \right) \tag{10}$$

where

T_S = the step change in ambient temperature,

t = the time elapsed since a step change in ambient temperature and,

τ_c = the time constant of the cable.

The phase (β) as a function of time (t) is from (3) and (10),

$$\beta = \frac{\omega_0^l}{v} + \frac{\omega_0^l \alpha T_S}{v} \left(1 - e^{-t/\tau_c} \right). \quad (11)$$

Therefore, from (11) and (5), the average frequency (f_n) in the first interval ($t_n, t_n + \tau$) is,

$$f_n = \left[\frac{\beta(t)}{\tau} \right]_{t_n}^{t_n + \tau} = \frac{1}{\tau} \left[\frac{\omega_0^l}{v} + \frac{\omega_0^l \alpha T_S}{v} \left(1 - e^{-t/\tau_c} \right) \right]_{t_n}^{t_n + \tau}, \quad (12)$$

and the average frequency (f_{n+1}) in the second interval ($t_n + \tau, t_n + 2\tau$) is,

$$f_{n+1} = \left[\frac{\beta(t)}{\tau} \right]_{t_n + \tau}^{t_n + 2\tau} = \frac{1}{\tau} \left[\frac{\omega_0^l}{v} + \frac{\omega_0^l \alpha T_S}{v} \left(1 - e^{-t/\tau_c} \right) \right]_{t_n + \tau}^{t_n + 2\tau}. \quad (13)$$

The absolute value of the difference between the average frequencies (f_n) and (f_{n+1}) is from (12) and (13),

$$\begin{aligned} |f_n - f_{n+1}| &= \left| \frac{\omega_0^l \alpha T_S}{\tau v} \left[2 e^{-\frac{t_n + \tau}{\tau_c}} - e^{-\frac{t_n}{\tau_c}} - e^{-\frac{t_n + 2\tau}{\tau_c}} \right] \right| \\ &= \left| \frac{\omega_0^l \alpha T_S}{\tau v} e^{-\frac{t_n + \tau}{\tau_c}} \left[2 - e^{-\frac{\tau}{\tau_c}} - e^{-\frac{\tau}{\tau_c}} \right] \right| \end{aligned} \quad (14)$$

Thus, the algorithm for the square root of the Allan variance of a signal passing through a transmission line having an exponential change in delay becomes from (1) and (14),

$$\sigma = \frac{\ell \alpha T_S}{\sqrt{2} \tau v} \sqrt{\frac{1}{N} \sum_{n=1}^N \left[e^{-\frac{t_n + \tau}{\tau_c}} \left\{ 2 - e^{-\frac{\tau}{\tau_c}} - e^{-\frac{\tau}{\tau_c}} \right\} \right]^2} \quad (15)$$

This equation is evaluated in Figure 5 for values of τ from 1 second to 10^6 seconds and variables $N=1$ to 10^7 , $\ell = 10$ meters, $\alpha = 10^{-5}/^\circ\text{C}$, $T_S = 10^\circ\text{C}$, $v = 2.1 \times 10^8$ meters per second and $\tau_c = 600$ seconds. These are estimated values for the case where 10 meters of cable are suspended in a rack cooled by plenum air and the door of the rack is opened.

These estimates indicate that the correction factor of the stabilization system will have to be between 10^3 and 10^4 , for a 10-km optical fiber link, in order to meet the goals.

Since no suitable commercial optical transmitters and receivers operating at 1300 nm wavelength are available, they are being developed at JPL. Circuitry for the cable stabilization system is also being developed. Prototypes of this equipment should be ready by the time the cable is installed in March of 1982.

A block diagram of the laser transmitter being developed is shown in Figure 6. It consists of the laser diode, a temperature stabilizer, an optical carrier level stabilizer and a modulation phase stabilizer.

The temperature of the laser is held near normal room temperature ($\approx 25^\circ\text{C}$). This stabilizes its operating characteristics and extends its life. It is purposely not cooled to below room temperature because water from the surrounding air would condense on the laser eventually causing problems. In the future we plan to seal the laser in an inert gas, in which case we could cool it to a lower temperature and the lifetime would be extended appreciably. Our goal of 50,000 hours mean time to failure appears to be readily achievable once the lasers go into full scale production and the bugs are worked out.

The optical carrier level stabilizer stabilizes the optical carrier power which tends to decrease with age for a given current.

The modulation phase stabilizer locks the phase of the detected output to the phase of the input signal.

There are two areas of concern at this time. Single-mode fiber directional couplers are not available and there is a problem coupling the laser output to a single-mode fiber efficiently.

PROGRESS

The optical fiber cable has been ordered and will be received in the first quarter of 1982.

Temperature coefficient of delay has been measured at JPL (reference 4) for various optical fibers. One result is shown in figure 7. The <7 ppm per $^{\circ}\text{C}$ shown is typical for fibers cabled in loose tubes, but can be much worse for tightly jacketed fibers. The indicated hysteresis is in the measurement system.

Tests were made to verify that the delay through single-mode optical fibers is affected very little by bending. A 500-MHz signal was transmitted through a 1-km piece of single-mode fiber cable. The phase delay through the cable was monitored while the cable was moved and bent in different ways. With a phase noise floor of about 0.2 degrees (1 ps) no change occurred that could be related to the movement of the cable.

The 1300 nm wavelength lasers and photodiodes were not available until May of this year (1981) and had to be packaged before they could be used. The packaging has just been completed.

A high isolation low-phase noise distribution amplifier and a temperature-stabilized phase detector, needed for the cable stabilization system, were developed in the meantime.

The distribution amplifier (reference 5) specifications are,

- * 25 to 225 MHz bandwidth,
- * 3 dB nominal gain,
- * +14 dBm output power,
- * Power spectral density of phase noise is < -140 dBc in a 1 Hz bandwidth, 10 Hz from a 100 MHz signal,
- * > 100 dB back to front isolation below 200 MHz and,
- * > 100 dB isolation between any pair of the 4 output ports up to 110 MHz.

The temperature-stabilized phase detector, Figure 8 (reference 6), uses a high-level Schottky diode mixer. It has a temperature coefficient of 0.014 ps/ $^{\circ}\text{C}$ or 8.7×10^{-6} radians/ $^{\circ}\text{C}$ at 100 MHz. The thermal time constant is ≈ 500 seconds. Good thermal control of these devices is achieved by winding the heater wire directly on the mixer and placing the thermistors at the most thermally sensitive location.

The control circuitry for the 1300 nm laser diode has been breadboarded and is being tested except for the modulation phase stabilizer. The laser diode is being simulated for these tests until the circuitry is proven.

A pin diode optical receiver design has been tested at 850 nm wavelength. It will be converted to 1300 nm wavelength when the 1300 nm laser diode is operating.

CONCLUSION

Preliminary measurements have been made on optical fiber cable, optical system components and phase-stabilization system components. The results indicate that the goals can be approached. There are some problems and some gray areas, but the technology is moving rapidly, and solutions are expected soon.

ACKNOWLEDGMENT

The author wishes to thank Richard Sydnor for technical assistance and suggestions throughout the course of this work.

REFERENCES

1. G. Lutes, "Optical Fibers for the Distribution of Frequency and Timing References," NASA Conference Publication 2175, Proceedings of the Twelfth Annual Precise Time and Time Interval (PTTI) Applications and Planning Meeting, held at Goddard Space Flight Center, Greenbelt, Maryland, Dec. 2-4, 1980.
2. K. Y. Lau, "Signal-To-Noise Ratio Calculation for Fiber Optics Links," The Telecommunications and Data Acquisition Progress Report 42-58, Jet Propulsion Laboratory, Pasadena, CA, Aug. 15, 1980.
3. Barnes, J. A., et al., "Characterization of Frequency Stability," NBS Technical Note 394, National Bureau of Standards, Washington, D.C., 1970.
4. L. Bergman, et al., Plots of Delay vs. Temperature, to be published, Jet Propulsion Laboratory, Pasadena, CA, 1982.
5. Y. V. Lo, "A Four-Way Distribution Amplifier for Reference Signal Distribution," The Telecommunications and Data Acquisition Progress Report 42-62, Jet Propulsion Laboratory, Pasadena, CA, April 15, 1981.

6. Y. V. Lo, "Temperature Stabilized Phase Detector," The Telecommunications and Data Acquisition Progress Report 42-64, Jet Propulsion Laboratory, Pasadena, CA, June 15, 1981.

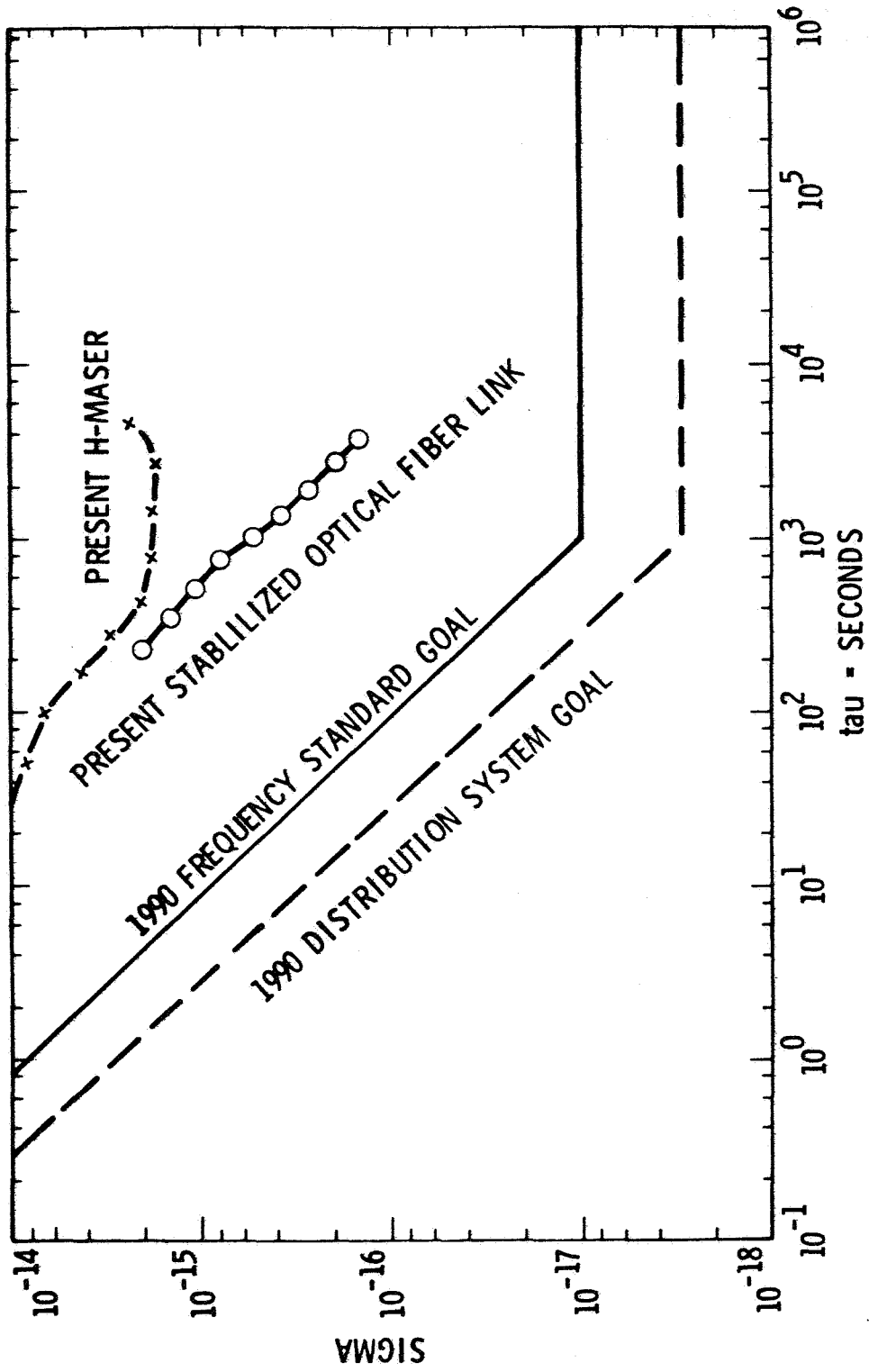


Figure 1. Present State-of-the-Art and Goals

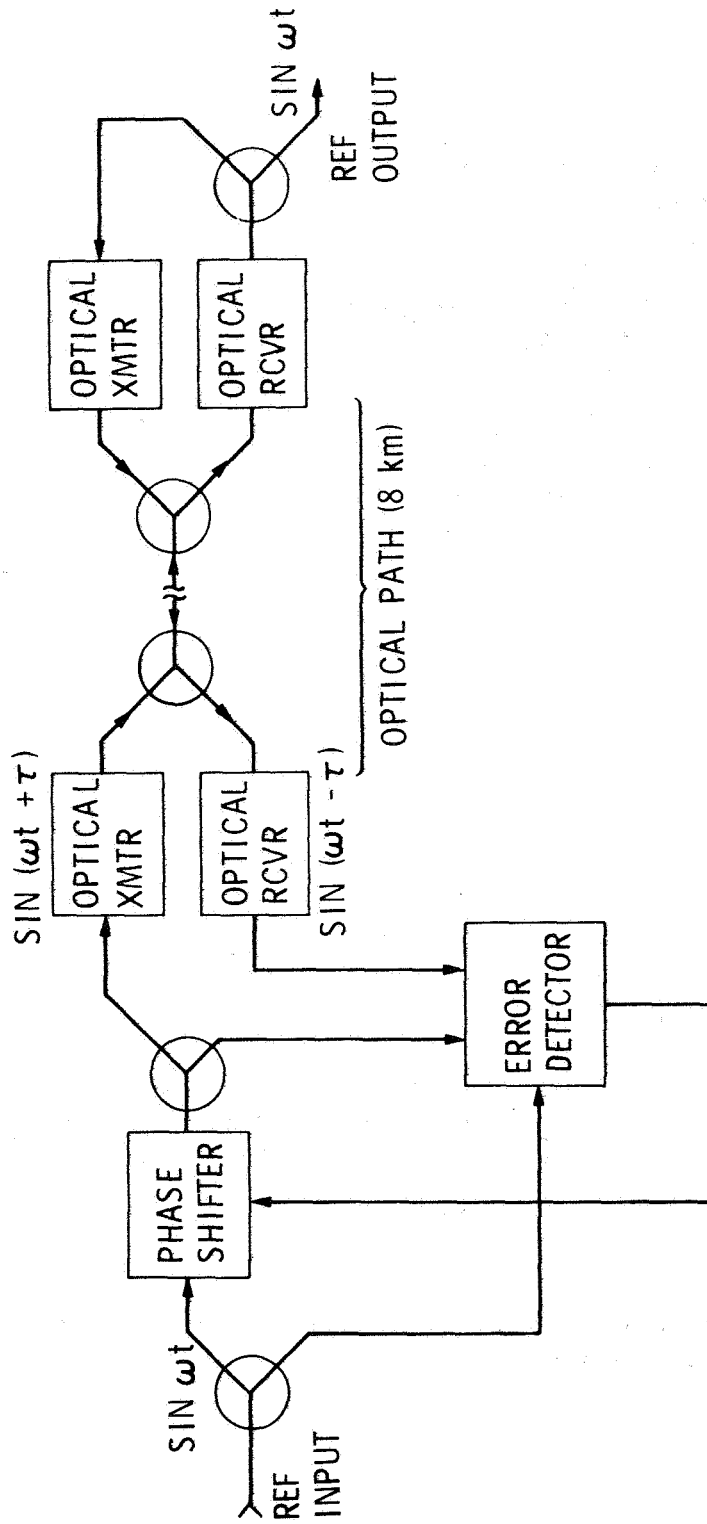


Figure 2. Conjugation Method of Phase Stabilization

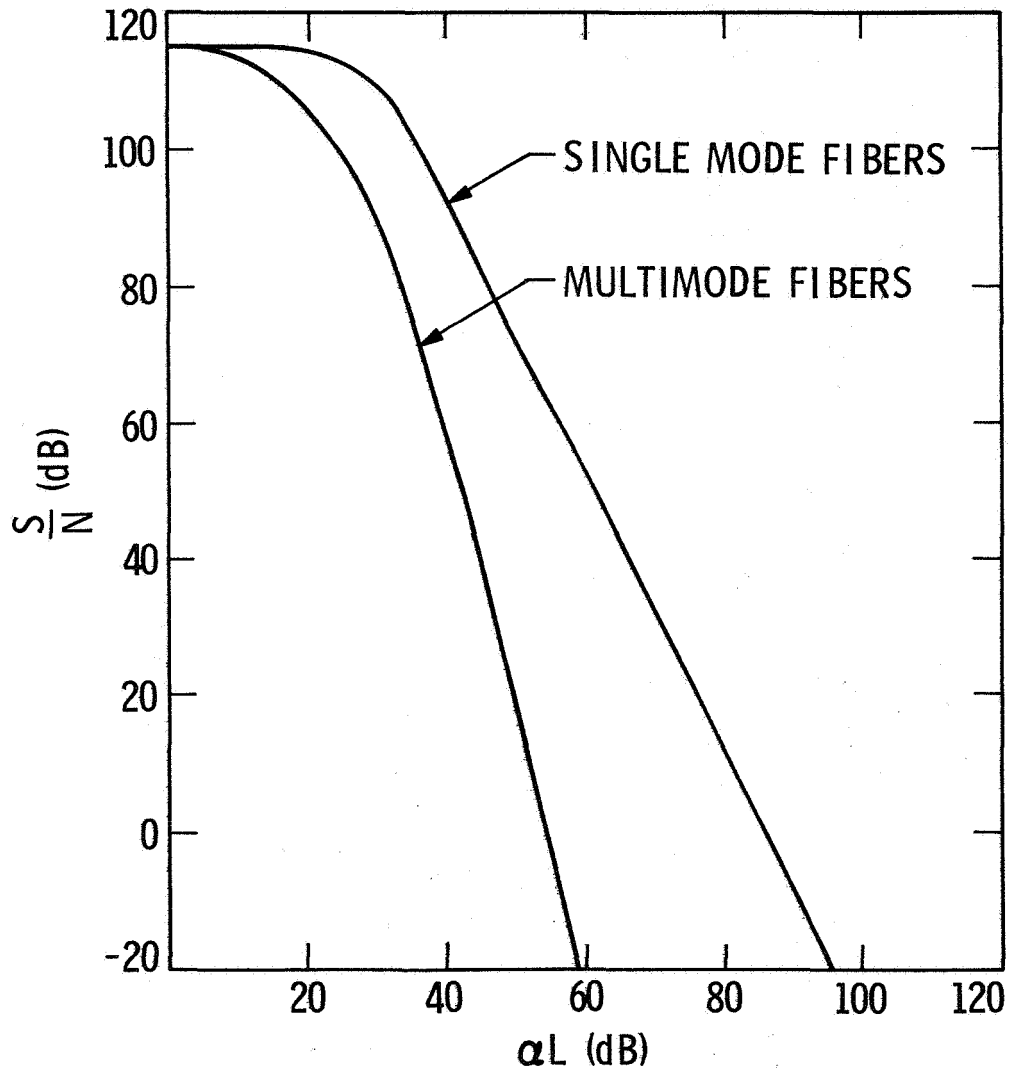


Figure 3. Signal-to-Noise Ratio vs Total Fiber Attenuation (10 Hz Bandwidth) at $F_o = 100$ MHz

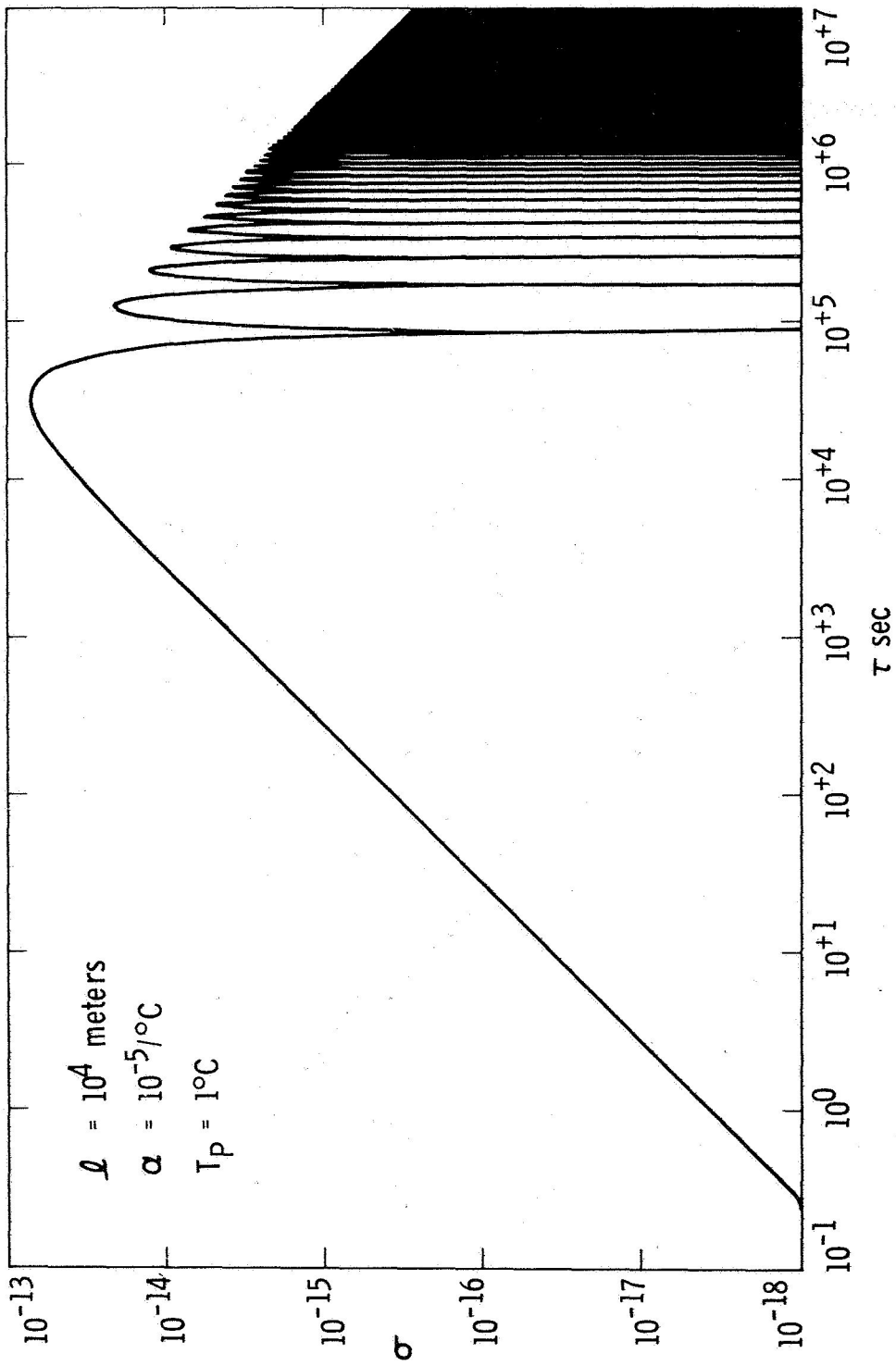


Figure 4. Estimated Frequency Stability vs Sampling Period for an Unstabilized Single Mode Optical Fiber Link

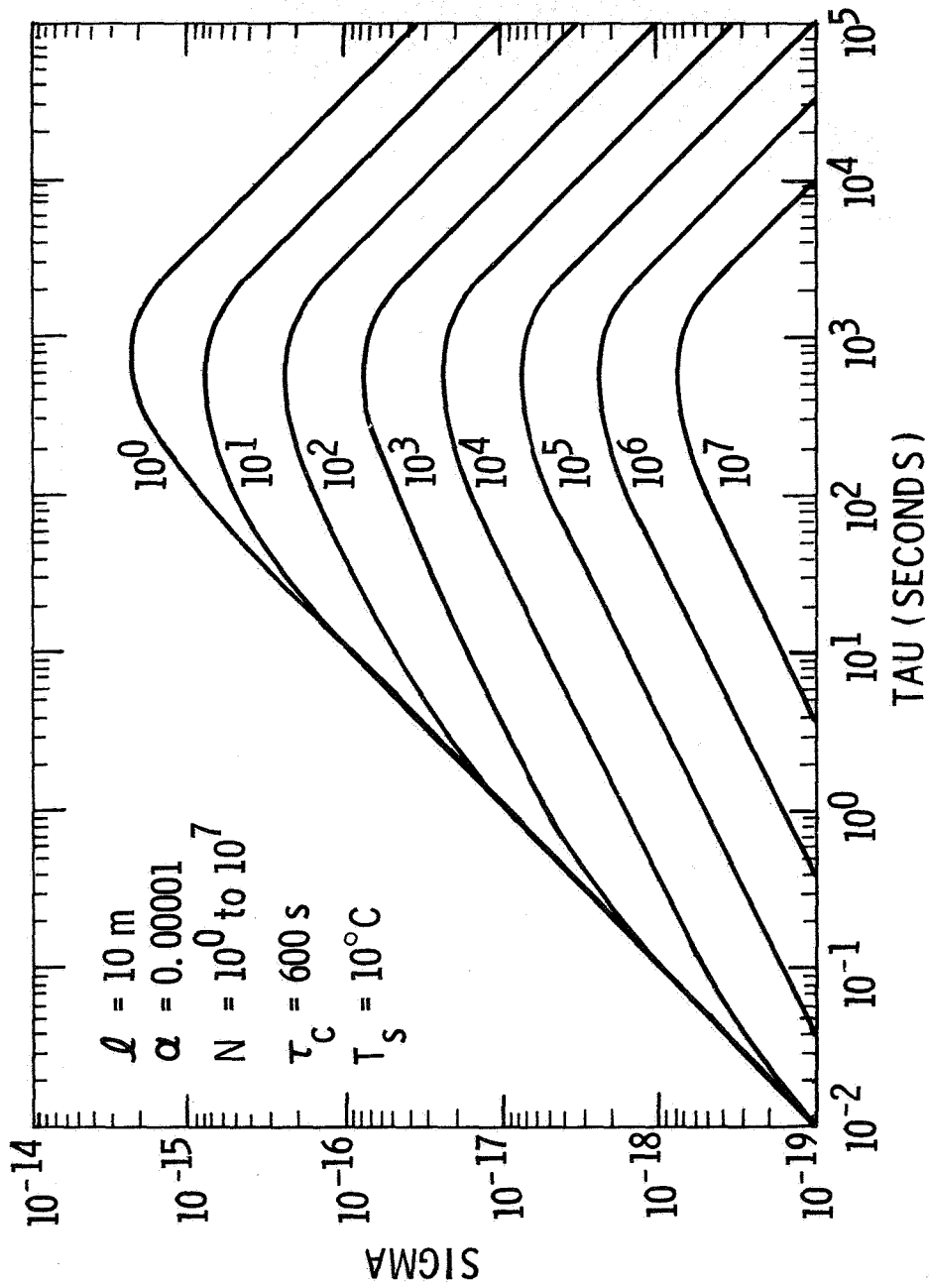


Figure 5. Stability as Affected by a Step Change in Temperature on a Cable

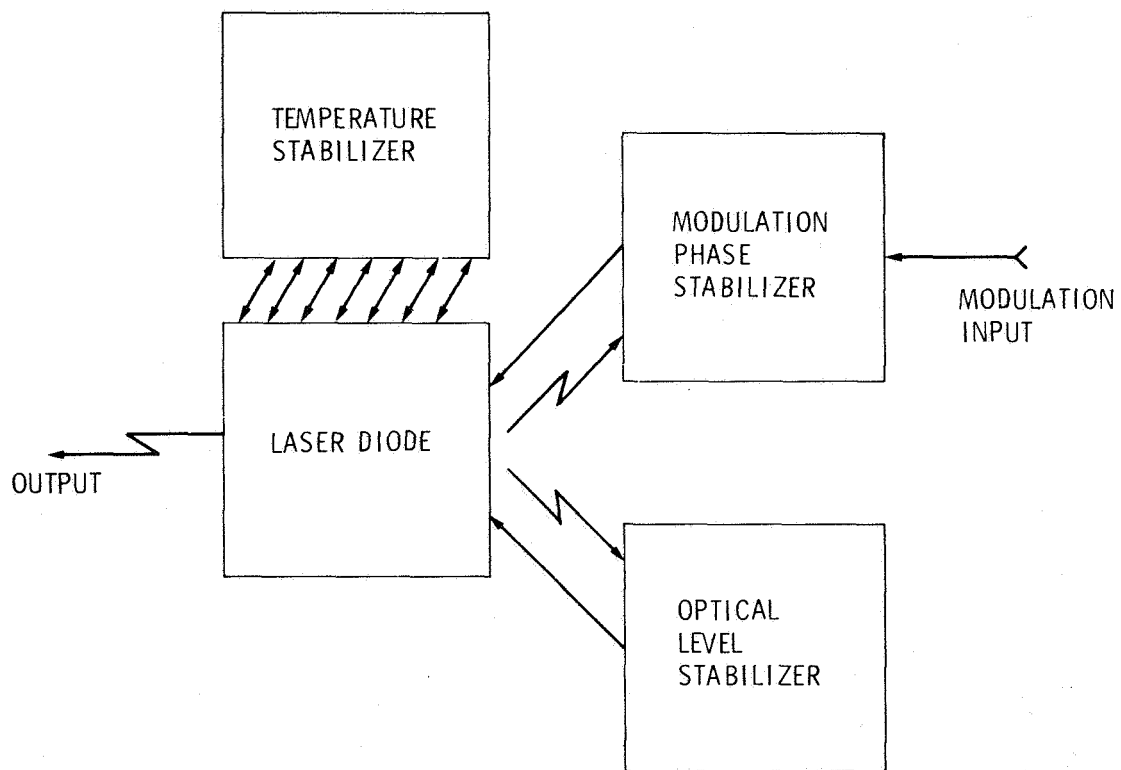


Figure 6. Block Diagram of the Laser Transmitter

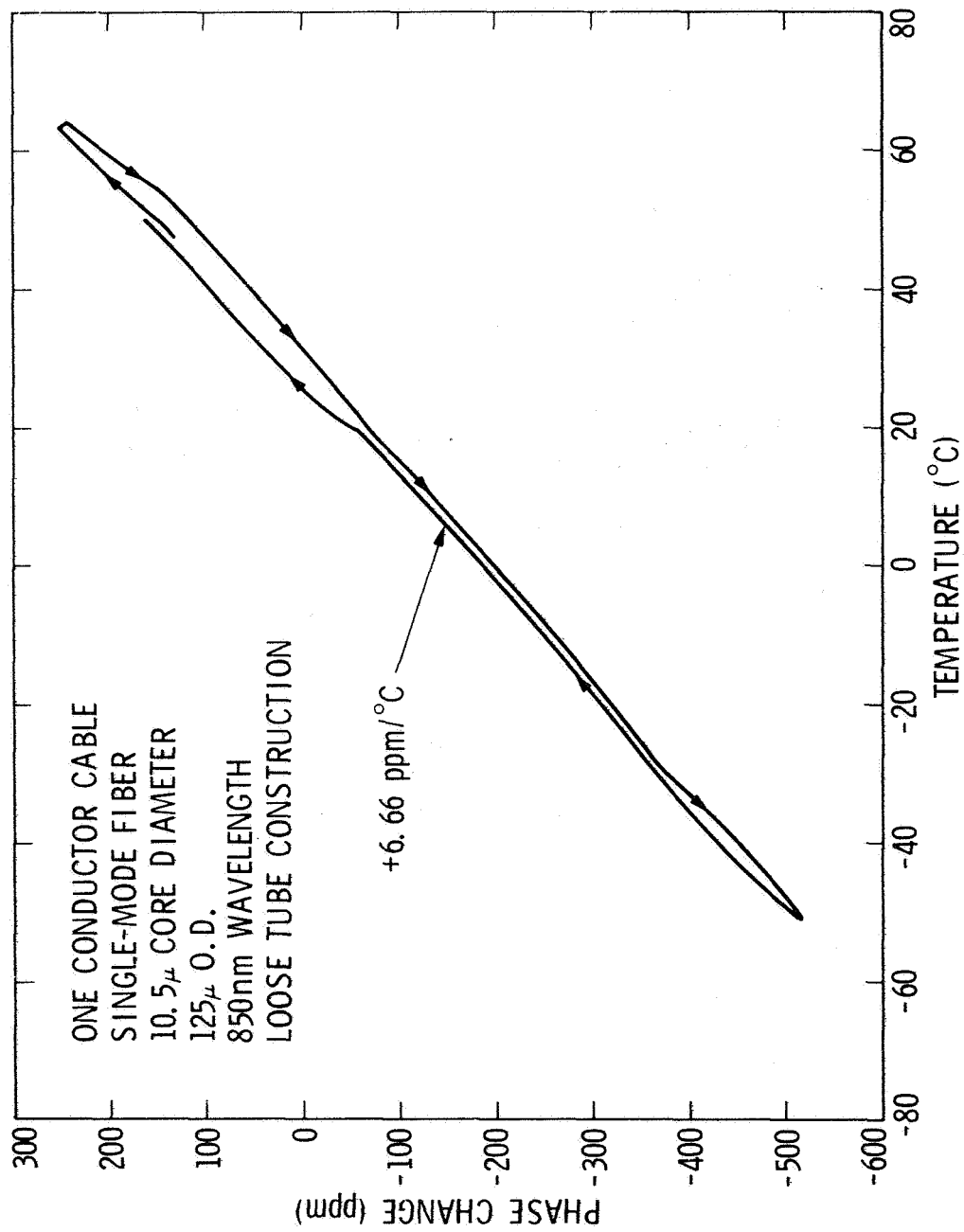


Figure 7. Phase Delay vs Temperature of a Single Mode Optical Fiber Cable

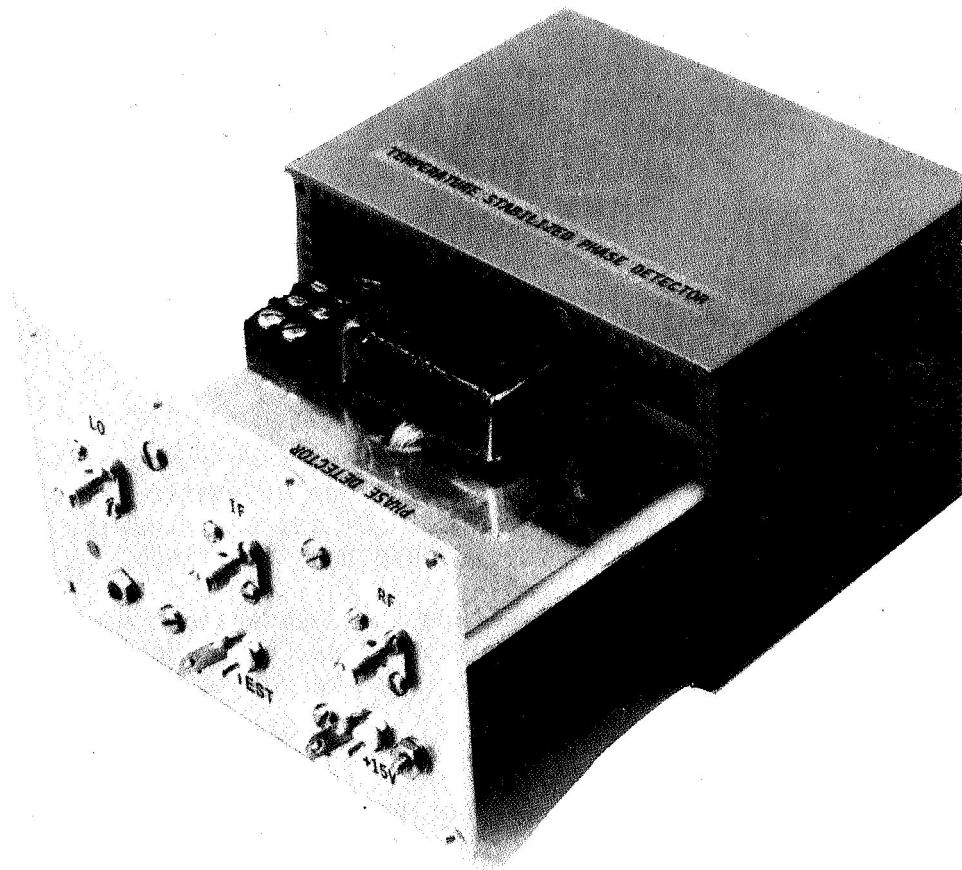


Figure 8. The Temperature Stabilized Phase Detector with the Insulation Removed